



Exogenous calreticulin improves diabetic wound healing

Matthew R. Greives, MD^{1*†‡}; Fares Samra, MD^{1†‡}; Savvas C. Pavlides, PhD^{2†}; Keith M. Blechman, MD^{1,3}; Sara-Megumi Naylor, MD^{1†}; Christopher D. Woodrell, MD²; Caprice Cadacio, MD²; Jamie P. Levine, MD³; Tara A. Bancroft^{2§}; Marek Michalak, PhD⁴; Stephen M. Warren, MD³; Leslie I. Gold, PhD³

1. Departments of Medicine and Pathology, New York University School of Medicine, New York, New York,
2. Department of Plastic Surgery, New York University School of Medicine, New York, New York,
3. Honors Program Medical Student, New York University School of Medicine, New York, New York, and
4. Department of Biochemistry, University of Alberta, Edmonton, Alberta, Canada

Reprint requests:

Dr. L. I. Gold, Department of Medicine and Pathology, New York University School of Medicine, 550 First Ave, NB 16E13, New York, NY 10016, USA.
Tel: +212 263 6320;
Fax: +212 263 7332;
Email: leslie.gold@nyumc.org

*Current address: Section of Plastic Surgery, University of Chicago.

†These authors contributed equally.

‡Participant of the Honors Program of the New York University School of Medicine.

§Participant of the Summer Undergraduate Research Program (SURP) of Sackler School of Graduate Biomedical Sciences.

Manuscript received: October 18, 2011

Accepted in final form: April 16, 2012

DOI:10.1111/j.1524-475X.2012.00822.x

ABSTRACT

A serious consequence of diabetes mellitus is impaired wound healing, which largely resists treatment. We previously reported that topical application of calreticulin (CRT), an endoplasmic reticulum chaperone protein, markedly enhanced the rate and quality of wound healing in an experimental porcine model of cutaneous repair. Consistent with these *in vivo* effects, *in vitro* CRT induced the migration and proliferation of normal human cells critical to the wound healing process. These functions are particularly deficient in poor healing diabetic wounds. Using a genetically engineered diabetic mouse (db/db) in a full-thickness excisional wound healing model, we now show that topical application of CRT induces a statistically significant decrease in the time to complete wound closure compared with untreated wounds by 5.6 days (17.6 vs. 23.2). Quantitative analysis of the wounds shows that CRT increases the rate of reepithelialization at days 7 and 10 and increases the amount of granulation tissue at day 7 persisting to day 14. Furthermore, CRT treatment induces the regrowth of pigmented hair follicles observed on day 28. *In vitro*, fibroblasts isolated from diabetic compared with wild-type mouse skin and human fibroblasts cultured under hyperglycemic compared with normal glucose conditions proliferate and strongly migrate in response to CRT compared with untreated controls. The *in vitro* effects of CRT on these functions are consistent with CRT's potent effects on wound healing in the diabetic mouse. These studies implicate CRT as a potential powerful topical therapeutic agent for the treatment of diabetic and other chronic wounds.

Failure to heal wounds, known as chronic wound healing, occurs in over 8 million people in the US.¹ Chronic nonhealing wounds are a consequence of various diseases including pressure ulcers, venous stasis ulcers, and diabetes.¹ The prevalence of diabetes mellitus, largely related to the surge in obesity, is 7.8% of the US population (23.6 million). Of the 200 million people worldwide who have diabetes (projected to reach 366 million by 2030), 15% develop chronic wounds, usually diabetic foot ulcers (DFUs), the most serious complication being amputation with an associated 2-year survival rate of 50–60%.^{2,3} DFUs largely result from autonomic neuropathy, causing loss of protective sensation, and also from peripheral arterial occlusive disease.¹ Chronic nonhealing wounds are a growing global health problem and have become a serious unmet medical need requiring major therapeutic intervention and are a significant economic burden.^{1,4}

Normal wound healing is a dynamic process partitioned into four essential phases^{4,5}: hemostasis/coagulation phase; inflammatory phase consisting of removal of dead cells and tissue; proliferative or tissue-forming phase involving migration and proliferation of fibroblasts into the wound, keratinocytes over the wound for reepithelialization, and neovascularization; and remodeling phase, characterized by matrix and matrix metalloproteinase (MMP) production by

ABAM	Antibiotic–antimycotic solution
BrdU	Bromodeoxyuridine
CRT	Calreticulin
DAPI	4,6-diamidino-2-phenylindole
db/db	Leptin receptor-deficient diabetic mouse model
DFU	Diabetic foot ulcer
DMEM	Dulbecco's modified Eagle's medium
ECM	Extracellular matrix
EG	Epithelial gap
EP	Epithelium
ER	Endoplasmic reticulum
FBS	Fetal bovine serum
FGF	Fibroblast growth factor
GT	Granulation tissue
HBSS	Hank's balanced salt solution
hpf	High-powered field
HMGB1	High-mobility group box 1
IACUC	The Institutional Animal Care and Use Committee
LRP1	Lipoprotein receptor-related protein
MMPs	Matrix metalloproteinase
PBS	Phosphate-buffered saline
PS	Phosphatidyl serine
TSP-1	Thrombospondin-1
VEGF	Vascular endothelial growth factor
wt	Wild type

fibroblasts, and finally, wound contraction. In contrast, chronic wounds lack this continuity of healing and are arrested in the inflammatory phase lasting more than 8 weeks, not healing, or recurring.⁴ These wounds have persistent infections, and the constant influx of inflammatory cells, which release cytotoxic enzymes, free oxygen radicals, and other inflammatory mediators, cytokines, and MMPs causes continued destruction of tissue and the accumulation of dead cells and tissue.^{1,5,6} In addition to these problems, diabetic wounds, largely DFUs, having defective cellular functions as a consequence of systemic disease, are the most difficult to heal of all chronic wounds. Particularly, diabetic wounds are defective in cell proliferation, the migration of cells into the wound including macrophage infiltration, extracellular matrix (ECM) production, clearance of dead tissue and apoptotic cells, and fibromyoblast differentiation.⁷ As a result, diabetic wounds are characteristically hypocellular, hypovascular, and have decreased granulation tissue (GT) formation, which is important in facilitating reepithelialization for wound closure. Whereas intensive research for novel topical therapeutic agents for impaired chronic and diabetic wound healing has long been underway, effective wound healing agents to heal these recalcitrant wounds are still not available.

Calreticulin (CRT) is a calcium-binding chaperone protein of the endoplasmic reticulum (ER) that functions in directing proper folding of proteins and in controlling many cellular functions through homeostatic control of cytosolic and ER calcium levels.⁸ Interestingly, CRT and other classic intracellular chaperones are emerging as proteins that also direct biological activities from the cell surface and extracellular space, thereby acting as important dual mediators of physiological and pathological processes including the immune response, phagocytosis, fibrosis, and tissue repair.⁹ We previously reported that topically applied CRT markedly enhances the rate and quality of cutaneous wound repair in a porcine model of experimentally induced partial and full-thickness wounds by affecting both the epidermis and dermis.¹⁰ In vitro, consistent with CRT's positive vulnerary effects and histological evidence of hypercellularity, abundant GT in the wound bed, and rapid wound resurfacing, exogenously added CRT-stimulated proliferation of human keratinocytes and fibroblasts and mediated concentration-dependent directed migration of these cells and of monocytes and macrophages, important in wound debridement.¹⁰ These data suggest that CRT might specifically correct the inherent defects of diabetic wound healing.

There is evidence for the involvement of CRT in nearly every phase of wound healing, and recent studies clearly show an important role for CRT in tissue remodeling.^{11,12} CRT expression is increased by many cell stress conditions including oxidative stress and hypoxia,^{8,13-15} which are significant in the wound environment. CRT is likely released by necrotic cells within an injured site and, as an initial involvement in wound healing, binds to the collagen-binding integrin $\alpha 2\beta 1$, on platelets¹⁶; CRT might regulate clot formation by this interaction.⁹ Released CRT interacts with matrix proteins and thereby regulates tissue remodeling.^{9,17,18} In addition, cell surface CRT is required for the engulfment of apoptotic cells and cancer cells by all phagocytes, which involves CRT association with phosphatidyl serine (PS), down-regulation of cluster of differentiation (CD)47 on the dead cells, and the binding of cell surface CRT on the dead cell to lipoprotein receptor-related protein (LRP1) on the phagocytes, for

signaling.^{19,20} Both the accumulation of destroyed tissue and cells and the lack of removal of this debris are major deterrents to wound healing and, particularly, in diabetic wounds, which often require multiple surgical debridement of nonviable tissue.

As the apparent effects of CRT on wound healing align with the known defects associated with diabetic wound healing,^{4,7,21-23} the current study was undertaken to determine whether CRT could improve the rate and quality of diabetic wound healing in vivo, using a genetically engineered leptin receptor-deficient diabetic mouse model (db/db). Furthermore, in vitro functions of CRT important in wound healing were performed using primary fibroblasts derived from these mice compared with wild type (wt). The data reported herein show that topical CRT directly improves the rate and quality of murine diabetic cutaneous wound repair, which is supported by its effects at the cellular level on fibroblast cell proliferation and migration, thereby suggesting that CRT has the potential to be used as an effective therapeutic agent for chronic wounds, including poor healing diabetic wounds.

MATERIALS AND METHODS

Materials

Recombinant His-tagged rabbit and human CRT were prepared as described²⁴ and used interchangeably; endotoxin was undetectable. CRT was stored in 10 mmol/L Tris containing 3.0 mmol/L calcium at pH 7.0 (termed buffer) to maintain the calcium binding molecule's proper conformation. Recombinant human fibroblast growth factor (rhFGF) was purchased from R and D Systems (no. 233-FB; Minneapolis, MN).

Diabetic murine wound model and treatments

The (*db/db*) leptin receptor-deficient mouse strain (BKS. *Cg-m+/+Lep^{db}*; Jackson Laboratories, Bar Harbor, ME, stock no. 000642) was used as a model for type II diabetes mellitus. The mice were acclimated to their environment for at least 1 week prior to wounding. The experimental protocol was approved by The Institutional Animal Care and Use Committee (IACUC) of New York University School of Medicine. For wounding, female mice (10–12 weeks old) were individually anesthetized by intraperitoneal injection of ketamine (75 mg/kg), xylazine (15 mg/kg), and acepromazine (2.5 mg/kg). Hair on the dorsum was removed by electric clipper followed by a depilatory agent. The wound area was sterilized with betadine and one full-thickness 6.0-mm excisional wound, patterned by a sterile punch biopsy, was made on each side of the dorsal midline using an iris scissor. The wounds extended through the dermis and *panniculus carnosus*. Ten microliters of CRT (5.0 mg/mL) in 10 mM Tris containing 3 mM calcium, vascular endothelial growth factor (VEGF) (1.0 mg/mL; 10 μ L/wound, as previously described)²⁵ (R&D Systems), as a positive control, or Tris-saline buffer (buffer: 10 mmol/L Tris, 150 mol/L NaCl, 3 mmol/L CaCl, pH 7.0), as a negative control, was applied to each wound. There were six mice per treatment. To prevent wound contraction, a silicone splint (0.5 mm thick; Grace Bio-Laboratories, Bend, OR) with a diameter twice the size of the wound was aligned around the wound according to the method of Galiano et al.²⁶

After treatment, the wounds were covered with an occlusive dressing (Tegaderm, 3M, St. Paul, MN) and the animals were placed in individual cages. The CRT and controls were applied to the wounds each day for the first 4 days following injury (total CRT, 200 µg; total VEGF, 40 µg) and redressed. Each mouse received the same treatment to avoid any systemic or crossover effect. The dressings were changed every 2 days throughout the time course. In one experiment, to determine whether CRT induced proliferation of cells in the wounds of the mice receiving CRT compared with buffer treatment, the mice were injected with bromodeoxyuridine (BrdU) intraperitoneally at 4 hours before euthanasia and tissue harvesting. Subsequently, these wound tissues were immunostained with an antibody to BrdU (Invitrogen, Carlsbad, CA) and proliferating cells quantified by light microscopy using three high-powered fields (hpfs) (200×) of the tissue sections, which were photographed followed by counting the cells within a defined area of the microscope lens (a boxed area); the values were averaged.

Histological preparation and morphometric analysis of the wounds

Time to closure

Digital photographs were taken of the wounds on the day of surgery and every day thereafter. Time to closure, defined as the time at which the wound defect was replete with new dermal tissue and skin fully apposed, was quantified by tracing the wound margin of the digital photograph with a fine-resolution computer mouse. The pixel area was determined using Sigma Scan Pro Image Analysis Version 5.0 digital analysis software (Aspire Software International, Leesburg, VA), and wound area was calculated as a percent of the original wound area, which was normalized to the splint representing a constant area. A completely closed gross wound, considered to be equal to its area, received a value of zero. There were six wounds per day.

Epithelial gap (EG)

The mice were euthanized and wound tissue was harvested on days 3, 4, 5, 7, 10, 14, 21, and 28 ($n = 6$ mice for each group) after injury. The wounds were analyzed for reepithelialization, defined as the reduction of the EG measured by light microscopy. Briefly, the wounds were excised, sectioned transversely (bisected) to allow measurement of the central part of the wound (remaining EG), fixed in 10% buffered formalin, and embedded in paraffin. The wound tissues, processed and stained with hematoxylin and eosin, were photographed using a mounted digital camera (Olympus, Melville, NY), images captured at 72 pixels/inch² and the distance between the advancing edges of keratinocyte migration (EG) over the wound bed quantified using SigmaScan software (San Jose, CA) (linear value in single dimension). Three serial sections were averaged for each wound. A completely reepithelialized wound was zero.

GT

The total area of the GT (wound bed/neodermis) was quantified by tracing regions of GT, as described earlier, for time

to closure. Tissue on the slides was stained with Masson trichrome stain to visualize collagen fibers (cyano) and cell nuclei (red) within the GT. The panorama tissue sections shown in Figure 1C were photographed using an Aperio ScanScope GL System (Aperio Technologies, Vista, CA) equipped with Aperio ImageScope Software at a magnification of 20×.

Treatment of cells with CRT

Cell culture

Primary human fibroblasts

Cells were obtained either from neonatal foreskin (New York University [NYU] School of Medicine institutional review board approval) or purchased as primary human adult low passage foreskin fibroblasts (CCD 1070SK; American Type Culture Collection, Manassas, VA). Fibroblasts were prepared from foreskin tissue samples by maceration in 1.0 mL of Librase 3 (Roche, Basel, Switzerland) for 1 hour. Following straining through a 70-µm sieve (BD Falcon, Bedford, MA), these cells or the 1070SK cells were cultured in Dulbecco's modified Eagle's medium (DMEM; Gibco/Invitrogen, Carlsbad, CA) containing 10% fetal bovine serum (FBS; HyClone, Logan, UT), and 1% antibiotic-antimycotic solution (ABAM, Mediatech, Manassas, VA). The DMEM contained a final concentration of either 1 g/L (4 mM) or 4.5 g/L (25 mM) glucose to simulate normoglycemic and hyperglycemic diabetic serum glucose levels.^{23,27,28} When 60 to 70% confluent, the cells were washed with phosphate-buffered saline (PBS), removed for replating with 0.25% trypsin-2.21 mmol/L ethylenediaminetetra-acetic acid (EDTA) (Mediatech), the trypsin neutralized with 10% FBS in DMEM, and the cells centrifuged and resuspended in complete DMEM containing the normal or high levels of glucose at the cell densities described in the assays below. The cells were cultured for at least 3 weeks in DMEM containing the two different glucose levels prior to use in proliferation and migration assays.

Primary murine fibroblasts

The following protocol was approved by the IACUC of NYU School of Medicine. Cells were isolated from adult (8–12 weeks old) C57/B16J wt and *db/db* murine depilated skin from the dorsum. Pieces (2.54 cm²) of full-thickness skin including the *panniculus carnosus* were stripped of fat and washed with PBS without Ca and Mg containing (2%) ABAM and placed in trypsin/EDTA (0.25%/1 mM) containing phenol red in Hank's balanced salt solution (HBSS) without Ca or Mg (Gibco, Invitrogen, no. 25200-056, Grand Island, NY) overnight at 4°C. The tissue, placed in 1.0 mL complete media composed of alpha-modified Eagle's medium with Earle's salts, without ribonucleosides and deoxyribonucleosides (Cellgro, Herndon, VA) containing 20% FBS, L-glutamine, and ABAM, was minced into fine pieces (<1.0 mm) with a curved iris scissor. Additional media were added slowly up to 5.0 mL, the tissue placed in a rotating shaker bath (New Brunswick Scientific Co. Inc, New Brunswick, NJ) at 37°C for 30 minutes, and then the cells were passed through a 70 µm sieve filter (BD Falcon, no. 352350), centrifuged at 1,530 rpm (Eppendorf, Hauppauge, NY Model 5403) for

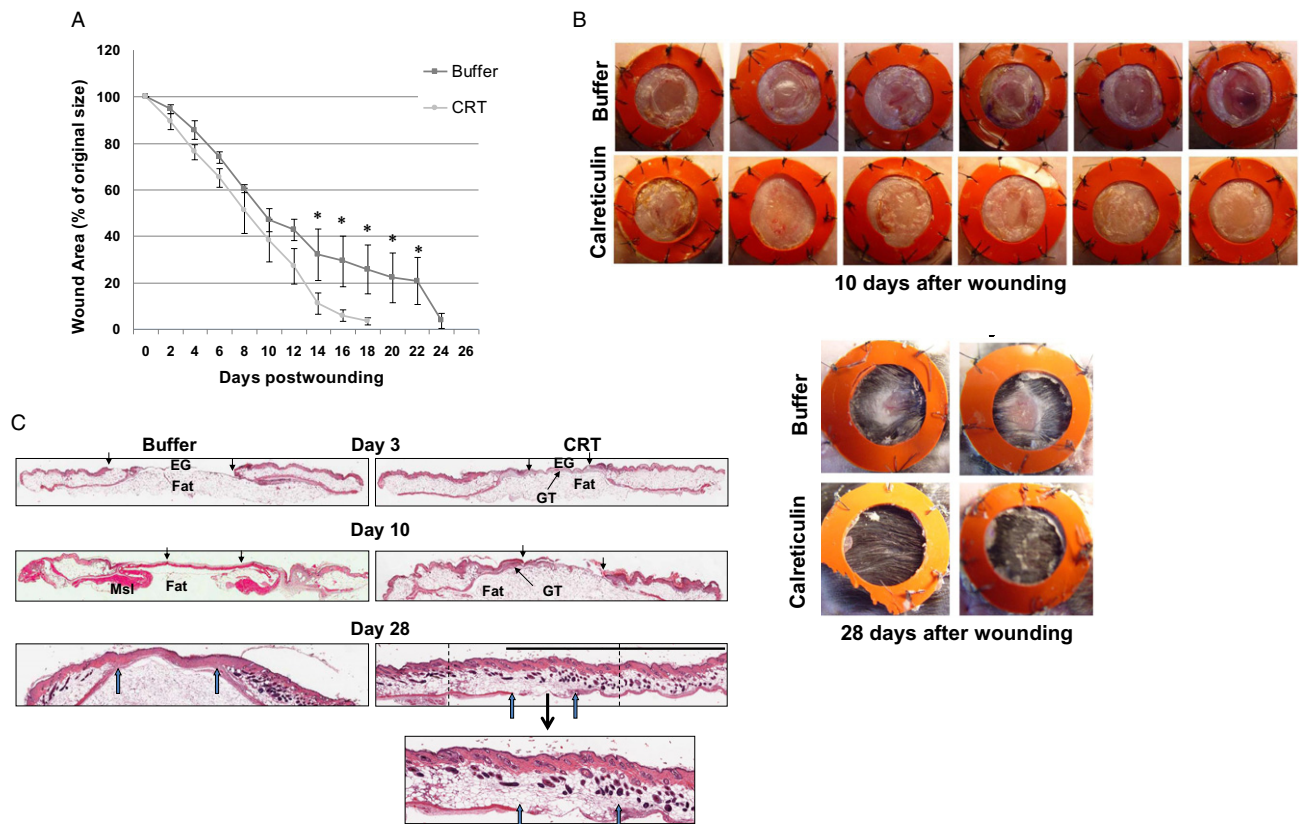


Figure 1. Calreticulin (CRT) enhances the rate of closure and improves the quality of cutaneous wound healing in a diabetic leptin receptor-deficient mouse (db/db; a model for type II diabetes mellitus). (A) Time to closure graph defined as the time the wounds were fully closed. Data were taken from daily digital photographs quantified as described ($n = 5$ wounds/treatment). (B) Diabetic db/db murine wound model, full thickness, 6.0 cm: CRT accelerates wound healing—gross images of diabetic (db/db) mouse wounds shown on day 10 and 28 postinjury. Full-thickness 6.0 mm excisional wounds were created on each side of the dorsal midline of the animal and following treatment with 10 μL of 5.0 mg/mL CRT, buffer, or vascular endothelial growth factor (VEGF) (positive control), a splint was placed over the wound as described in detail in the materials and methods section. The mice were treated every day for 4 days (two wounds/mouse, $n = 6$ mice in total). Wounds 10 days postwounding (top panel) and 28 days postwounding (bottom panel). (C) CRT accelerates wound healing—histology of diabetic mouse wounds shown at days 3, 10, and 28 postwounding. Wounds were prepared and stained with hematoxylin and eosin as described in the materials and methods section. CRT-treated wounds exhibit earlier wound maturity than the buffer-treated wounds throughout repair. Downward black arrows denote the epithelial gap (EG) between the migrating epithelium. Green upward-facing arrows denote the previously cut interrupted *panniculus carnosus*. Buffer-treated wounds (left); CRT-treated wounds (right). Magnification: 20 \times (28 days wound expanded by approximately twofold by computer zoom). GT, granulation tissue; Msl, muscle.

6 minutes at 4°C, washed, centrifuged, seeded on 60 mm *Primaria* plates (BD Falcon) and grown to 60–70% confluency prior to replating (approximately 2 weeks). These cells can be repassaged six to eight times, frozen in liquid nitrogen in complete media and 10% dimethyl sulfoxide (DMSO), thawed, and replated with 80% viability.

In vitro assay for cellular proliferation

Primary human (CCD 1070SK) or murine dermal db/db and C57/Bl6J fibroblasts were seeded on 96-well plates (BD Falcon) at a density of 2×10^3 /well in their respective complete media. The human fibroblasts were cultured in normal or high

glucose as described earlier. Both the mouse and human cells were grown until 50–60% confluent (approximately 48 hours) and switched to media containing 0.5% serum for 24 hours. Increasing concentrations of rabbit or human CRT were added to the cells and fibroblast growth factor (FGF; 5.0 ng/mL) or 5% FBS and 0.5% FBS served as positive and negative controls, respectively. Treatments were performed in triplicate. After 48 hours, 20 μL of (3-(4,5-dimethylthiazol-2-yl)-5-(3-carboxymethoxyphenyl)-2-(4-sulfophenyl)-2H-tetrazolium (MTS) solution (CellTiter96 assay, G3580, Promega, Madison, WI) was added, and absorbance was read at 490 nm (Bio-Rad 680, Benicia, CA). Percent growth stimulation was determined by averaging the relative units of measurement in the wells treated with CRT or FGF compared with the negative

controls. Preliminary experiments utilized a wider range of doses to determine optimal range.

Cellular migration

Wound healing scratch plate assay

Primary human dermal fibroblasts were seeded in 24-well tissue culture plates (BD Falcon) at 2.0×10^4 /well and the primary murine diabetic (db/db) and C57/BIJ6 wt fibroblasts were seeded in 24-well *Primaria* tissue culture plates at 3.0×10^4 /well. Both cell types were grown in their respective complete media until approximately 70–80% confluent. Wounds were created down the center of each well with a 200- μ L plastic pipet tip and the wells washed with PBS to remove displaced cells. A fine-tipped marker was used to denote the edges of the artificial wound on the underside of each well. Increasing concentrations of CRT in media were added to each well in triplicate. FBS at 0.5% and at 5% served as negative and positive controls, respectively. To visualize the cells, at time zero, three wells were stained with 1.0 mL 0.025% Coomassie blue stain in 10% acetic acid, 45% methanol for 15 minutes. The experiment was terminated at 24 hours by incubating the remaining wells with the stain, the wells washed with PBS and the cells viewed under an inverted light microscope (Axiovert s-100; Zeiss, Thornwood, NY). Images were captured and cell migration was calculated by measuring the area (pixels) unoccupied by cells compared with the area of the original scratch at zero time using Metamorph software version 7.1.3.0 (Molecular Probes, Eugene, OR). As a control, all plates were normalized with respect to cell density at a part of the plate distal and lateral to the scratch. Initial experiments were performed in the presence of 5 μ g/mL mitomycin C, and as previously shown,¹⁰ proliferation did not contribute to the migratory response.

Thin membrane chamber cellular migration assay

The thin polycarbonate membrane ChemoTx system (8.0 μ m pore size, Neuroprobe Inc., Gaithersburg, MD) was used to determine concentration-dependent directed migration in response to CRT compared with positive and negative controls as shown. The human fibroblasts, diabetic db/db and C57/BIJ6 wt murine fibroblasts were used, and the assay was performed as described.¹⁰ The lower part of the chambers was filled with a range of CRT concentrations as well as 5.0 ng/mL rhFGF as the positive control in 330 μ L. All treatments were prepared in the media specific for each cell type, as described earlier, and each dose was performed in triplicate. Fibroblasts and adherent macrophages were washed with PBS, removed from the plates with 0.25% trypsin-2.21 mmol/L EDTA in HBSS (Cellgro), the cells centrifuged at $235 \times g$ for 5 minutes, and pellets suspended in serum free media. The frame was placed on top of the wells and 50 μ L of cell suspensions were placed on the membrane above each well. Human and murine fibroblasts were used at a cell density of 5×10^4 /well and were incubated for 4 hours. Following incubation at 37°C and 5% CO₂, membranes were washed with PBS, fixed in 4% paraformaldehyde for 5 minutes, removed from the apparatus, and applied to coverslips. The cells were stained using VECTASHIELD and

4,6-diamidino-2-phenylindole (DAPI; Vector Laboratories, Burlingame, CA). Each membrane was photographed at 200 \times magnification in at least six fields and an average of three hpf was calculated for the number of cells/well using Kodak ID software (Kodak, Rochester, NY).

Statistical analyses

For morphometric analysis of the area of GT formation, the distance of EG, and the time to complete closure of the wounds, the data were measured in pixels and presented as a mean \pm standard error with units of pixels² (area), pixels (distance). The number of cells staining for BrdU in the wound tissues and the number of DAPI-stained fibroblasts and macrophages within the ChemoTx membranes was quantified/counted and the data expressed as number of cells per hpf (=200 \times) in at least three fields. Values in pixels obtained from images of the unclosed wound area in the scratch plate assay were obtained and subjected to analysis of variance. Statistical analyses were performed using SigmaStat Statistical Software Version 2.03 (Aspire Software International). Statistical significance was defined as $p < 0.05$ and was determined with unpaired two-tailed *t*-tests. These statistical assays were applied to all experiments and were performed using GraphPad Prism version 4.02 (GraphPad Software, La Jolla, CA).

RESULTS

CRT enhances the rate of closure and improves the quality of cutaneous wound healing in a diabetic mouse model

Gross wounds

In contrast to human cutaneous wound healing, mice heal by contraction of the *panniculus carnosus*, a muscle layer beneath the dermis. To more closely simulate human healing, mouse wounds were held open by a silicone stent,^{25,26} which allows GT formation and epithelial migration. By convention, we assessed wound healing by three major criteria: time to complete closure, rate of reepithelialization (resurfacing), and GT formation (neodermal remodeling) in experimental and control groups. Time to closure is dependent on the latter two criteria. Because impaired wound healing related to human diabetes mellitus is characterized by specific physiological cellular defects as a result of systemic disease,^{4,7,21,22} we chose a leptin receptor genetically null mouse (db/db) with physiological characteristics of diabetes mellitus type II (hyperglycemia, obesity, hyperinsulinemia, impaired wound healing) to determine whether CRT treatment of full-thickness excisional wounds could improve impaired healing of diabetic wounds. Following an initial dose-escalating study, the optimal dose of CRT that induced the fastest reepithelialization measured as the smallest remaining nonepithelialized wound area or EG and greatest area of GT in the wound bed, measured as dermal area, was 5.0 mg/mL (50 μ g/day for 4 days, total 200 μ g/mL). Figure 1A illustrates that there is a statistically significant decrease in the average wound size/area (*) in the CRT-treated wounds compared with the buffer-treated control on day 14 postinjury until full closure was achieved in the CRT-treated wounds by 17.6 days

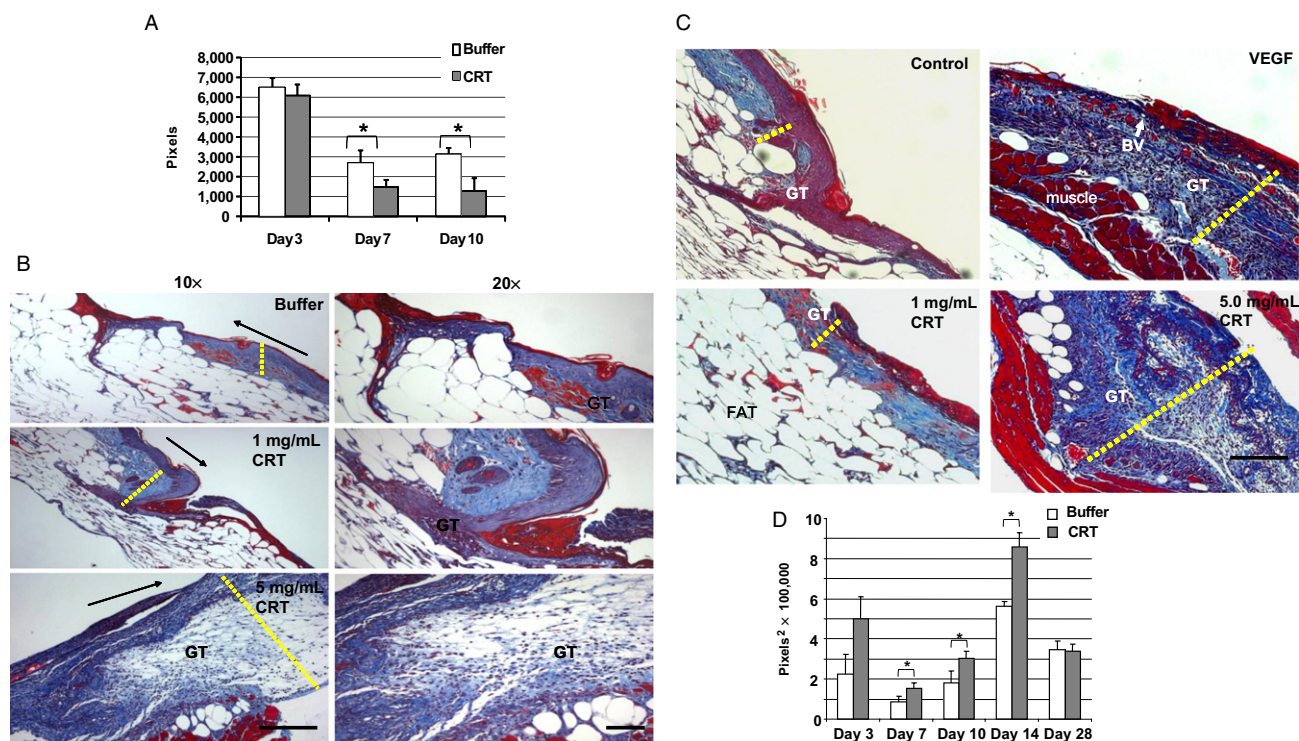


Figure 2. Calreticulin (CRT) induces faster wound reepithelialization and increases granulation tissue (GT) formation in diabetic db/db mice. (A) Epithelial gap: CRT induces faster closure of epithelial gap. The distance between the advancing edges of keratinocyte migration over the wound bed was quantified on days 3, 7, and 10 postwounding, as described: day 3, $n = 6$ for CRT and $n = 3$ for buffer; day 7, $n = 6$; day 10, $n = 6$. (B) Day 4: CRT dose-dependently increases GT formation—4 days postinjury. Wound tissues were stained with Masson trichrome: collagen fibers (cyano) and cell nuclei (red) are observed within the GT. Top (left, right) panels: buffer; middle (left, right) panels: CRT 1.0 mg/mL; bottom (left, right) panels: CRT 5.0 mg/mL. Direction of migrating epithelium is indicated by a black arrow. Depth of the GT is marked by a dotted yellow line perpendicular to the wound surface. Magnification: left panels, 160x; right panels, 320x of same tissue. (C) Day 7: CRT dose-dependently induces greater GT than buffer-treated or vascular endothelial growth factor (VEGF)-treated wounds—7 days postwounding. Wound tissue was prepared as in (B). Photomicrographs of wounds were taken at 7 days postwounding. Top left panel: buffer control; top right panel: VEGF; bottom left panel: CRT 1.0 mg/mL; bottom right panel: CRT 5.0 mg/mL. Magnification: 160x. (D) Granulation tissue (dermal area): CRT induces greater GT. The total area of GT in the wound bed/neodermis was quantified on days 3, 7, 10, 14, and 28 postwounding on hematoxylin and eosin-stained tissues as described in the materials and methods section ($n = 6$ /time point/treatment (except day 3, buffer, $n = 3$ experiments). BV, blood vessels.

compared with 23.2 days for the buffer control ($p \leq 0.045$; $n = 6$ /treatment) wounds. These calculations were based on the average of the day postinjury that each wound was completely filled with new tissue and grossly fully closed. Therefore, CRT induces wound closure 5.6 days earlier than the buffer-treated controls. Differences in the gross wounds could be observed at 3, 7, 10, 14, 21, and 28 days postwounding as shown by the histology of the wound on day 3 postwounding in Figures 1C and 2A. The increased rate of closure of the CRT-treated (bottom panels) compared with the buffer-treated control (top panels) wounds is clearly shown by photographs of representative gross wounds at 10 days after injury in which the epithelium (EP) of the CRT-treated wounds appears intact compared with the buffer-treated control (Figure 1B, top panel) and at 28 days postinjury in Figure 1B (bottom panel; $n = 6$ mice). It is notable that the CRT-treated wounds at 28 days postinjury display full-length black hair within the stent surrounding the original wound (bottom panel).

Quantitative and qualitative analysis of wounds: EG and GT formation

Migration of the keratinocytes over the wound, for reepithelialization, and ample GT formation are critical early markers for both qualitative and quantitative assessment of successful wound healing. As shown in Figure 1C, the histological analysis of the wounds is consistent with the increased rate of wound closure of the CRT-treated wounds compared with the buffer-treated controls. As early as 3 days after wounding, the entire CRT-treated wound contains GT (upward black arrow; right panel) and the distance of migrating EP (demarcated by downward black arrows in all panels) from the wound margin creates a smaller EG in the wound bed center compared to the buffer-treated control (left). By day 10 postwounding, the EG is reduced in the CRT-treated (right) wounds and the GT area is greater compared with the buffer-treated controls (left). The margins of the wounds are marked by green upward arrows

showing the interrupted *panniculus carnosus* that was made during wounding. As observed by light microscopy, both the CRT and buffer-treated wounds were reepithelialized (but not closed) by day 14 (not shown). By 28 days postwounding (Figure 1C; Supporting Information Figure S1), the quality of the CRT-treated (right) wound tissue more closely resembles adjacent unwounded skin than the buffer-treated wounds (left). Interestingly, epidermal appendages, including abundant normal-appearing hair follicles, are observed in the CRT-treated wound bed. The interruption in the *panniculus carnosus* (green arrow) is the only evidence of the original wound ensuring that the unusual and unexpected regrowth of hair follicles is in the area of prior excisional wounding.

The graph in Figure 2A shows that the EG is significantly smaller in the CRT-treated compared with the buffer-treated controls on days 7 ($p \leq 0.039$; $n = 6$) and 10 ($p \leq 0.012$; $n = 6$) postinjury. As illustrated in Figure 2B, at 4 days postwounding, a dose-dependent increase in GT formation was observed in the CRT-treated wounds (middle [left and right] and bottom [left and right] panels) compared with the buffer-treated controls (left and right top panels). Figure 2B at 4 days (bottom right) and, particularly in Figure 2C, at 7 days postwounding (middle right panel) illustrate the depth and hypercellularity of the GT/neodermis, which is largely composed of fibroblasts synthesizing ECM proteins. As shown in Figure 2C, the buffer-treated wounds (top left panel) and the lower concentration of CRT-treated wounds (middle left panel; 1.0 mg/mL) are much less cellular (red) and contain less collagen (cyano) than both the VEGF (top right panel) and CRT-treated wounds (bottom right panel), indicating a dose-response with respect to cellularity and collagen in the CRT-treated wounds. However, CRT treatment did not appear to increase the number of blood vessels compared with VEGF (upper right panel compared with top right panel; white arrow). Quantitative measurement of the area of GT of the wounds (Figure 2D) indicated that the GT area was significantly increased in the CRT-treated wounds on day 7 ($152,226 \pm 27,816$ vs. $87,624 \pm 25,773$ pixels² $p \leq 0.001$) and day 10 ($301,418 \pm 36,244$ vs. $181,924 \pm 58,200$; $p \leq 0.001$), which persisted through day 14 ($857,108 \pm 73,784$ vs. $564,014 \pm 23,982$ pixels² $p = 0.004$). The extent of GT of the CRT-treated compared with the buffer-treated wounds did not reach statistical significance on day 3 postwounding due to animal death or infection in the buffer-treated control ($n = 3$ wounds). By day 28 postwounding, the extent of neodermis was similar in the CRT-treated compared with the buffer-treated wounds.

CRT induces cellular recruitment, cellular proliferation, and collagen synthesis in murine diabetic wounds

The consequences of diabetes in impaired chronic wound healing at the cellular level have been well characterized.^{4,7,21,22,27,29} These functions appear to be overcome by CRT treatment of the murine diabetic wounds, which we show here (Figure 3A) are highly cellular, implicating both recruitment of cells into the wounds (migration) and cell proliferation to populate the well-healing wounds. Compared with buffer-treated wounds, which are largely composed of fat and a paucity of GT (top right panel), the CRT-treated wounds were highly cellular with ample GT, which was evident by day

3 postwounding, as illustrated in Figure 3A (top left panel). With higher magnification, cell types appear to be macrophages (red arrows), leukocytes (yellow arrows), fibroblasts (green arrows; bottom right panel)—collagen fibrils are shown (cyano stain, black arrows). Furthermore, CRT application to the wounds induced proliferation of cells in the wounds as shown by the mice that received injections of BrdU. At 10 days postwounding BrdU staining is present in the basal and suprabasal keratinocytes of the epidermis and numerous cells that appear to be fibroblasts, in the neodermis (Figure 2B). Table 1 illustrates a statistically significant increase in the number of epidermal and dermal cells in the CRT-treated compared with the buffer-treated mouse wounds analyzed on day 3 postwounding (44.1 ± 2.86 , $n = 5$ wounds compared with 23.6 ± 4.75 cells per hpf $n = 3$ wounds; $p \leq 0.0036$).

Exogenous CRT stimulates proliferation and induces migration of murine dermal fibroblasts isolated from diabetic mice

We show here that topical CRT clearly enhances the rate and quality of wound repair in the genetically diabetic murine model (db/db) consistent with the profound effects observed on wound histology. However, direct effects of CRT on the proliferation and migration of diabetic cells in vitro would provide a cellular level explanation for how CRT improves diabetic wound repair. Therefore, we developed a novel method to isolate adult dermal fibroblasts from the diabetic (db/db) and wt mice to compare the effect of CRT on proliferation and migration, in vitro. As shown by the graph in Figure 4A, CRT dose-dependently stimulates proliferation of wt murine fibroblasts with a statistically significant peak response of 1.53-fold over the untreated control at 0.5 ng/mL ($p \leq 0.0001$). At this CRT concentration, the response of the db/db fibroblasts is not significant at 1.17-fold over the control; the difference between the wt and db/db cell response at this concentration is significant ($p \leq 0.0007$). The db/db fibroblasts are less sensitive with a peak response at 100 ng/mL representing a 1.27-fold increase over the control ($p \leq 0.0026$). Both wt and diabetic fibroblasts respond with higher magnitude to 10% serum at 1.99 ($p \leq 0.0001$) and 1.68-fold ($p \leq 0.0001$) over the untreated control, respectively ($n = 4$).

The db/db murine fibroblasts were compared with wt fibroblasts for their migratory response to CRT using the scratch plate in vitro wound healing assay and in a concentration-dependent directed manner, using a thin membrane chamber assay. The differences in morphology of the wt compared with db/db fibroblasts are notable in Figure 4B and C, respectively. The nuclear to cytoplasmic ratio appears higher in the wt cells than the db/db cells, giving a false impression of higher cell density in the former; the db/db nuclei appear pyknotic and the cells more round. Figure 4D reflects the wound closure data shown in Figure 4B and C. As shown by the graph in Figure 4D ($n = 4$ experiments), 24 hours following CRT treatment of wounded fibroblasts, a decrease in motility of the db/db fibroblasts is illustrated by their inability to close the wound to the same extent as the wt fibroblasts. The diabetic cells require two times more CRT (100 ng/mL compared with 50 ng/mL) than the wt cells for a peak migratory response to achieve 57.6% ($p \leq 0.017$) compared with 87.4% wound closure ($p \leq 0.0009$; $n = 4$ experiments),

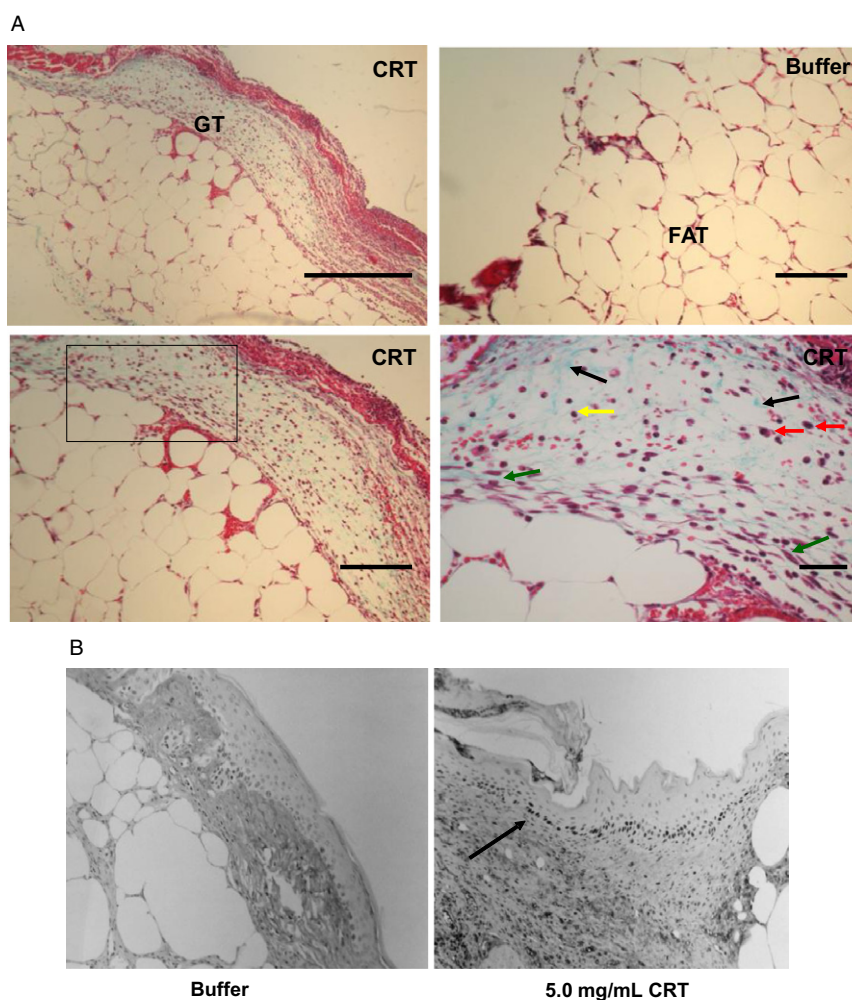


Figure 3. Calreticulin (CRT) induces cellular recruitment, cellular proliferation, and collagen in murine diabetic (db/db) wounds. (A) Day 3: CRT induces a highly cellular granulation tissue. The photomicrographs of CRT-treated wound tissue stained with trichrome at 3 days postwounding. Top left, bottom left and bottom right panels: CRT 5.0 mg/mL; top right panel: buffer control. Bottom right panel: macrophages (red arrows), leukocytes (yellow arrows), and fibroblasts (green arrows). Bottom (left, right) panels: collagen fibrils (cyano stain, black arrows). Magnification: top left panel: 114x; top right and bottom left panels: 160x; bottom right panel: 320x. (B) CRT induces cellular proliferation. The mice were injected with bromodeoxyuridine (BrdU) 4 hours before harvesting the wounds and the tissue immunostained with anti-BrdU. The wounds are shown at 10 days postwounding. Left panel: buffer control; right panel: CRT 5.0 mg/mL, photomicrograph shows BrdU in basal and suprabasal keratinocytes of the epidermis (black arrow) and in cells of the dermis. Magnification: 160x.

respectively. Wound closure for db/db fibroblasts at this peak of activity (50 ng/mL) is 56% ($p \leq 0.00004$). CRT at 50 ng/mL induced 18% more wound closure/migration of wt fibroblasts than 5% FBS (Figure 4D; $p \leq 0.0021$). In addition, the db/db fibroblasts respond less well than the wt to the serum positive control (45.7% vs. 69.5%; $p \leq 0.000058$). Taken together, whereas the db/db fibroblasts show a statistically significant increase in wound closure with CRT treatment at the peak response (100 ng/mL), the cells are both less sensitive and show a less robust response than their wt counterpart.

As shown in Figure 4E, using a chamber assay, CRT induces concentration-dependent directed migration of murine wt

fibroblasts, which is maximal at 10 ng/mL CRT giving a 4.2-fold increase in migration over the untreated control ($p \leq 0.0136$; $n = 3$ experiments). At 10 ng/mL CRT, the db/db cells are 2.14-fold less sensitive than the wt ($p \leq 0.034$). In contrast, the migratory response of the db/db cells is 10-fold less sensitive than the wt cells with a peak response at 100 ng/mL CRT, which was 2.8-fold over the buffer control ($n = 3$; $p \leq 0.0041$). Interestingly, CRT induces a greater migratory response than the FGF positive control in wt and db/db fibroblasts in this assay (3.3-fold for the wt [$p \leq 0.063$]). Again, the db/db cells have a weaker response to FGF than the wt fibroblasts ($p \leq 0.101$). According to these data, whereas the db/db fibroblasts are less sensitive to CRT

Table 1. Quantification of proliferating cells by immunohistochemical analysis of bromodeoxyuridine (BrdU) incorporation in diabetic db/db murine wounds at 3 days postwounding

	Buffer	Calreticulin
Cells/hpf	23.58	44.14
SE	4.75	2.86

Mice were injected with BrdU intraperitoneally at 4 hours before harvesting the wounds. The wound tissue was processed on slides and subsequently immunostained with an antibody to BrdU for quantification of proliferating cells by light microscopy, as described in the materials and methods section. Three high-powered fields (200 \times) of the tissue sections were photographed, the cells counted within a boxed area, and the values averaged. Calreticulin induced a statistically significant increase in the number of epidermal and dermal cells in the wounds compared with buffer-treated control (44.1 ± 2.86 , $n = 5$ compared with 23.6 ± 4.75 , $n = 3$; $p \leq 0.01$) cells per high-powered field.

and mount a less robust migratory response, CRT appears to functionally correct the migratory defect.

Exogenous CRT stimulates proliferation of human dermal fibroblasts and induces migration of human dermal fibroblasts cultured in high glucose

To determine whether human dermal fibroblasts grown under conditions that simulate serum glucose levels of hyperglycemic diabetic patients would have blunted proliferative and migratory responses to CRT, similar to the murine db/db fibroblasts, we used an established model for inducing a diabetic phenotype in cells to compare with those cultured in normal glucose.^{23,27,28} As shown in Figure 5A, whereas CRT dose-dependently stimulated proliferation of fibroblasts in normal glucose, with a peak response of 1.9-fold over the untreated control at 1.0 ng/mL (untreated vs. treated, $p \leq 0.025$; $n = 3$ experiments; similar to the FGF control), human fibroblasts in high glucose barely respond to both CRT and FGF (1.2 compared with untreated control at 1.0, 10, and 50 ng/mL).

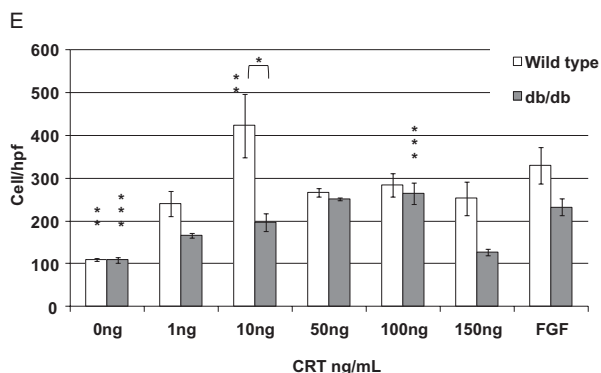
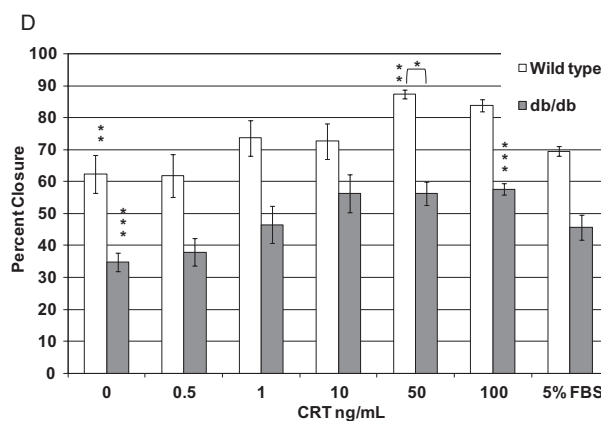
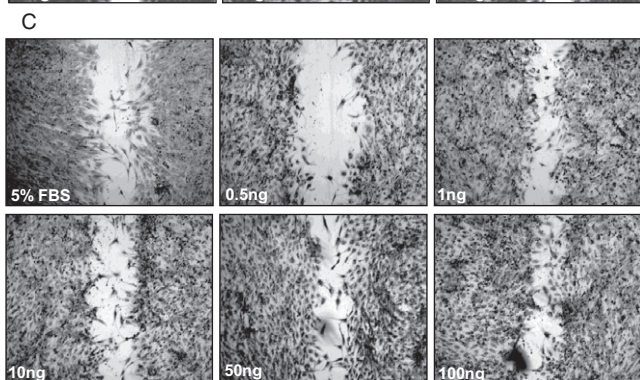
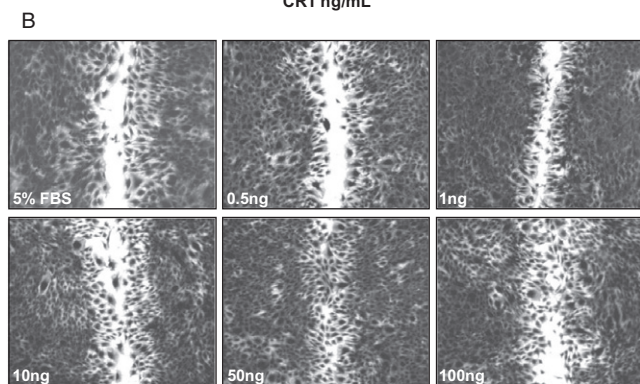
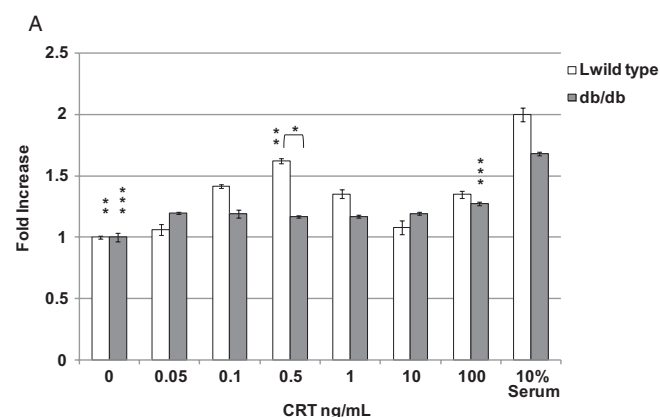
Using the wound healing scratch plate assay, as shown in Figure 5B, CRT dose-dependently stimulates the migration of the human "diabetic" fibroblasts with a peak response at 50 ng/mL, achieving 88% wound closure (compared with untreated control, $p \leq 0.0001$), whereas the peak response of fibroblasts in normal glucose is 50 times more potent yielding 92% closure at 1.0 ng/mL (compared with untreated control, $p \leq 0.0004$; $n = 5$ experiments [one representative experiment is shown]). Interestingly, fibroblasts in both high and normal glucose had a greater response to CRT than to 5% FBS (CRT compared with FBS: 92% vs. 67% [for normoglycose]; 88% vs. 83% [high glucose]). Similar results were obtained using the chamber migration assay. Figure 5C shows that CRT induces a dose-dependent increase in the number of fibroblasts that migrated through the membranes with a peak response of 10 ng/mL for the cells grown under

normal glucose (compared with untreated control, $p \leq 0.033$) and at 150 ng/mL for those in high glucose (compared with untreated control, $p \leq 0.0007$). At 10 ng/mL CRT, 63% less fibroblasts in high glucose migrated to CRT than those in normal glucose (3.5-fold compared with 12-fold over the untreated control $p \leq 0.030$; $n = 5$ experiments). Similar to the experiments using the scratch plate assay, the fibroblasts in normal glucose responded more strongly to CRT than 5.0 ng/mL FGF (8.8-fold vs. 4.9-fold over untreated control, respectively; $p \leq 0.035$), whereas the diabetic simulated fibroblasts respond nearly equally to both CRT and FGF at 4-fold and 5.5-fold, respectively, over untreated control.

DISCUSSION

A lack of agents that can treat the severe complications associated with poor healing of cutaneous wounds in patients with diabetes mellitus remains despite the current understanding of differences in the physiology of healing in normal vs. diabetic wounds. DFUs, the most common wound complication of this disease, largely result from both neurologic and vascular complications and overlying opportunistic infections that persist due to defective wound healing.³⁰⁻³² In the current study, we used the leptin receptor-deficient diabetic mouse as a paradigm to directly test the efficacy of CRT in impaired diabetic wound healing. Of the many murine models of diabetic healing, following excisional wounding, the db/db mouse has been shown to be most severely impaired, providing a longer window of time to test new therapeutic agents for poor wound healing.³³ In addition, the splinted wounds prevented wound contraction through the *panniculus carnosus* muscle located immediately below the dermis and provided more suitable model for human cutaneous wound healing whereby the histology of wound reepithelialization and GT formation could be observed and measured.²⁶ Similar to previous studies using the db/db mouse,³³ full wound closure in the untreated mouse was attained by day 23.2 postexcisional wounding. In contrast, the wounds in the mice treated with CRT for the first 4 days after wounding, closed an average of 6 days earlier at 17.6 days postwounding. Whereas all wounds were resurfaced with EP by day 14 after wounding, the difference in gross wound closure (total skin apposition) between the CRT-treated and untreated wounds was statistically significant each day after day 14 ($p \leq 0.045$).

The most remarkable morphological difference between CRT- vs. buffer-treated db/db mouse wounds is that the former exhibit more advanced healing both at day 10 after wounding, when the wounds are resurfaced, and at day 28, when the wounds are healed with full normal length hair. Low-power microscopy revealed that the CRT-treated wounds have formed GT on top of many layers of fat by 3 days postwounding. This is in sharp contrast to the thick layer of fat shown in the EG between the migrating epithelial tongues at days 3 and 10 postinjury in the control wounds. Moreover, newly formed collagen fibrils and abundant cellularity were already observed by day 3 postwounding, and the histology of the wounds shown at 4, 7, 10, and 28 days postwounding is consistent with their mature wound macroscopic appearance. Both the reduction in EG, indicating greater keratinocyte migration, and an increase in GT formation in CRT-treated



wounds were statistically significant over controls through day 10 postwounding for EG and through day 14 in measurements of extent of GT. Similar to the previous porcine studies, in the current study, we showed a statistically significant increase in proliferating keratinocytes, specifically in the suprabasal and basal layers of the stratified epidermis, and in fibroblasts in the CRT-treated mice compared with the control after *in vivo* labeling with BrdU. Finally, abundant hair follicles with normal length hair were observed at the 28 days postwounding time point. Whereas regrowth of epidermal appendages, such as hair follicles and sweat glands, does not occur in adult mammals following removal of full-thickness skin,³⁴ wounding of mouse skin has been shown to induce an embryonic regenerative state in the skin conducive to hair follicle neogenesis via the wingless integration (Wnt) pathway.^{35,36} These studies suggest that the follicles within the

wound bed originate from epithelial cells (nonhair follicle stem cells) and undergo an embryonic type of hair follicle development through epithelial–mesenchymal interactions. However, the new hair follicles lacked melanocytes (i.e., white hair in black mice) and follicle neogenesis required a minimum wound size of 2.25 cm.³⁵ It is doubtful that the buffer-treated wounds lacked hair at day 28 because of their lag in healing compared with the CRT-treated wounds. Thus, the black hair growth in our study implicates a novel function of CRT to induce hair regrowth and other epidermal appendages following cutaneous full-thickness damage. Further experimentation is necessary to understand the role of CRT in induction of stem cell-derived hair follicle growth.

The dynamic specific spatial and temporal expression of endogenous CRT suggests that this protein plays a

Figure 4. Exogenous calreticulin (CRT) stimulates proliferation and induces migration of murine dermal fibroblasts isolated from diabetic (db/db) mice. (A) Murine fibroblast proliferation: CRT stimulates proliferation of murine db/db and wild-type (wt) fibroblasts; db/db cells are less sensitive. Fibroblasts, isolated from the dorsal skin of db/db and wt mice, were grown to confluency, trypsinized and reseeded onto 96-well plates as described in the materials and methods section. The cells were treated with increasing concentrations of CRT (0.05 ng/mL–100 ng/mL) and after 48 hours, cell proliferation was determined using the CellTiter 96 MTS assay as described. Growth stimulation was determined by averaging the relative units of measurement as fold increase of CRT-treated cells or 10% serum-treated cells (positive control) over the negative control of 0.5% fetal bovine serum (FBS) (value of 1.0). All treatments were in triplicate ($n = 4$ experiments). Statistical significance (p -values) compares wt vs. db/db at peak CRT activity for wt (0.5 ng/mL) ($*p \leq 0.0007$); wt untreated vs. CRT peak activity (0.5 ng/mL) ($**p \leq 0.0001$); db/db untreated vs. at peak CRT activity (100 ng/mL) ($***p \leq 0.0026$). (B–D) CRT dose-dependently induces migration of murine wt and diabetic db/db primary fibroblasts in a scratch plate assay; the magnitude of the response is less in db/db cells. Murine dermal fibroblasts were plated in 24-well Primaria tissue culture plates, grown to 70–80% confluency, cells switched to 0.5% serum, wounded with a pipette tip, and then treated with increasing concentrations of CRT (0.5 ng/mL–100 ng/mL) all as detailed in the materials and methods section. At 0 hours, and after 24 hours, the experiment was terminated by adding 0.025% Coomassie blue stain. Wound closure was determined by capturing images and determining the open area compared to the original scratch at time zero, all as described in the materials and methods section. (B) Murine wt fibroblasts; (C) murine diabetic fibroblasts. Increasing concentrations of CRT are show in each panel. Five percent FBS is positive control. The panels represent one experiment included in the graph (D). The percent closure of the wound on the plate is reflected in the graph ($n = 4$ experiments). Statistical significance (p -values) compares wt vs. db/db at wt peak CRT activity (50 ng/mL) ($*p \leq 0.00004$); wt untreated vs. CRT (50 ng/mL) ($***p \leq 0.0009$); db/db untreated vs. CRT peak activity (100 ng/mL) ($***p \leq 0.017$). (E) CRT induces concentration-dependent migration of murine WT and db/db fibroblasts in a chamber assay. Increasing concentrations (1–150 ng/mL) of CRT were added to the bottom chambers of a thin polycarbonate membrane ChemoTx chamber migration system, the cells added to the top of the membrane, and the cells incubated for 4 hours as described in the materials and methods section. The membranes were stained with VECTASHIELD and 4,6-diamidino-2-phenylindole, photographed, and the number of migrating cells averaged for three high-powered fields (hpf) as described. The experiments were performed in triplicate ($n = 3$ experiments). The values are described cells/hpf. Statistical significance (p -values) compares wt vs. db/db at peak CRT activity for wt (10 ng/mL) ($*p \leq 0.034$); wt untreated vs. CRT at peak activity (10 ng/mL) ($**p \leq 0.0136$); db/db untreated vs. CRT at peak concentration (100 ng/mL) ($***p \leq 0.004$). FGF positive control is at 5 ng/mL.

physiological role in the wound repair process. Similar to the porcine wound healing study, we observed the identical temporal and spatial changes in CRT expression in db/db murine wounds (Supporting Information Figure S2). Whether the change of expression of CRT in wounds is due to changes in the intracellular chaperone function of CRT, known to be a stress response protein^{8,9} and/or receptor-driven responses from the outside in, we propose that CRT normally plays a positive role in wound healing and that the additional amount of CRT applied to the experimental animal wounds induces its strong vulnerary effect.

Released CRT has been shown to interact with numerous constituents of the ECM including collagens, laminin, and thrombospondin (TSP)-1, which when tethered to the ECM modify cell functions including fibronectin and MMP expression for tissue remodeling.^{9,17,18} Collagen and fibronectin are important components of GT, contributing to its integrity and delivery of tethered growth factors. Using CRT null mouse embryo fibroblasts (lethal at embryonic day 13.5), it has recently been reported that CRT is important in collagen I and III transcription, trafficking through the ER, release, and deposition into the ECM through a calcium-sensitive mechanism.¹² Importantly, these studies show that CRT complexes with collagen intracellularly and plays critical roles in multiple stages of collagen expression and processing. However, the addition of exogenous CRT had no effect on collagen release in the CRT null or wt murine embryonic fibroblasts. This result is inconsistent with the increased effect of topical CRT on collagen induction in vivo shown herein by trichrome and picrosirius red staining (unpublished data) in both the porcine¹⁰ and murine studies shown here. In addition, we

show that CRT induces a dose-dependent increase in collagen type I and fibronectin in cell lysates of adult human primary dermal fibroblasts in vitro (unpublished data). The discrepancy in induction of collagen by exogenous CRT may be related to differences between the undifferentiated embryonic cells vs. adult fibroblasts and/or species-specific effects and in vivo to the presence of other accessory proteins and cells. These results imply that factors in vivo may play a role in collagen induction through cell surface receptor signaling. Further in vivo and in vitro studies with different cell types are necessary to determine whether exogenous CRT directly functions to stimulate collagen release.

The molecular pathogenesis of impaired wound healing in patients with diabetes mellitus, largely related to hyperglycemia, causes multiple dysfunctions at the cellular level.^{1,4,7,21,22,29} Diabetic fibroblasts show a lack of response to the hypoxic conditions of the wound microenvironment in the functions of migration, proliferation, and production of cytokines, leading to insufficient GT.²² In addition, infection and subsequent biofilm formation is a major problem due to lack of macrophages to phagocytose bacteria.^{1,6} The abundant and cellular GT composed of proliferating cells (by BrdU uptake) in the CRT-treated db/db mice compared with the wt suggested that CRT might directly affect these important cellular functions that are critically deficient in the poor healing of diabetic wounds. Because CRT was shown to induce proliferation and migration of normal human fibroblasts in vitro,¹⁰ the current studies were directed at determining whether exogenous CRT could correct these reported defects^{21,37} in diabetic fibroblasts by comparing mouse primary db/db and wt fibroblasts for their responsiveness to CRT. We show that

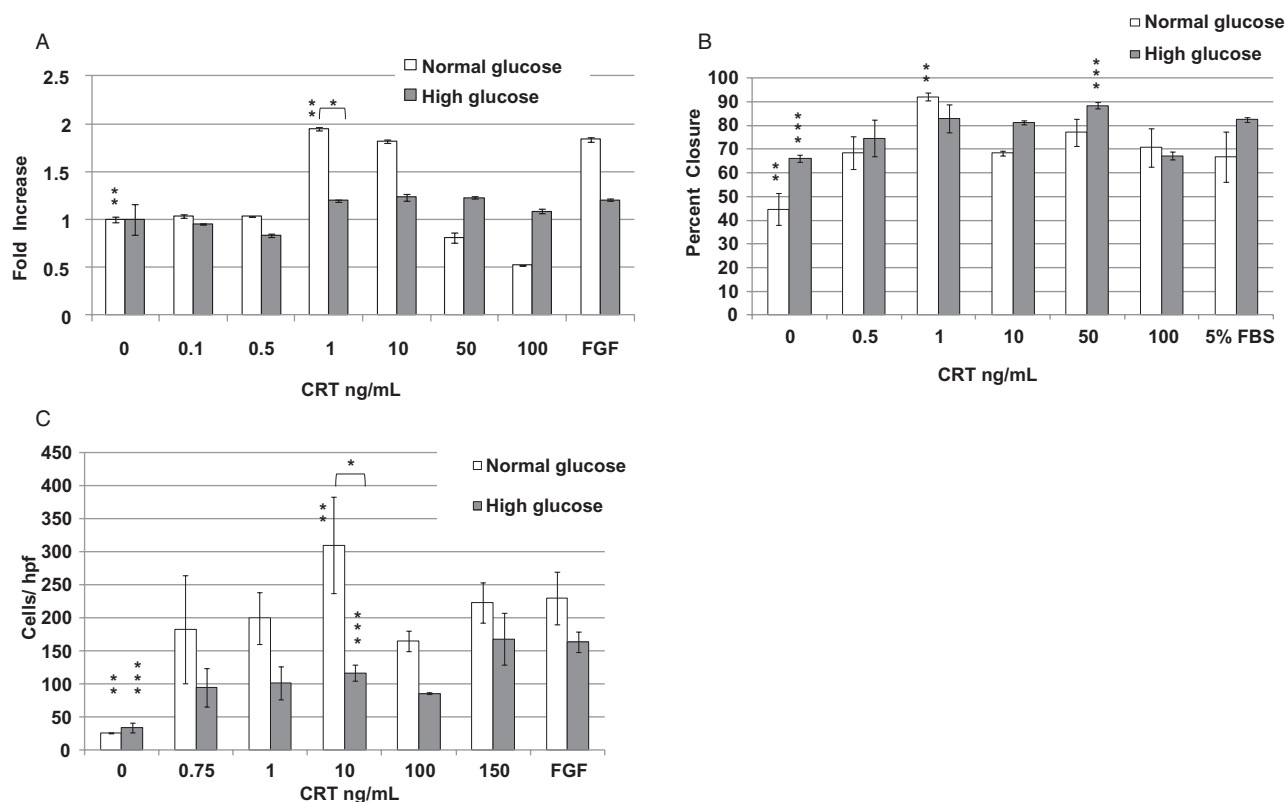


Figure 5. Exogenous calreticulin (CRT) stimulates proliferation and induces migration of human dermal fibroblasts cultured in high glucose. (A) Human fibroblast proliferation. CRT induces proliferation of fibroblasts grown in media containing normal levels of glucose but not those grown under high glucose levels. Primary human fibroblasts were grown in tissue culture in media containing normal levels of glucose (4 mM) or high glucose (25 mM) to simulate hyperglycemic serum levels of type II diabetes, as described in the materials and methods section.^{23,27} The cells were reseeded into 96-well plates at 2×10^3 /well in media containing the two glucose levels, synchronized, treated with increasing concentrations of CRT (0.1–100 ng/mL) for 24 hours and cell proliferation determined using the MTS assay as described in the materials and methods section. Experiments were performed in triplicate ($n = 3$ experiments). Statistical significance (p -values) compares fibroblasts grown in normal glucose vs. fibroblasts grown in high glucose at peak CRT activity for normal (1.0 ng/mL) ($*p \leq 0.0001$); normal untreated vs. CRT (1.0 ng/mL) ($**p \leq 0.0249$). Fibroblast growth factor (FGF) positive control is at 5 ng/mL. (B) Human fibroblast migration/scratch plate assay. Human fibroblast grown in normal or high glucose migrates in response to CRT in an in vitro wound closure scratch plate assay. Primary human dermal fibroblasts were plated, wounded, treated with increasing doses of CRT (0.5–100 ng/mL) and assayed for wound closure 24 hours later as described in the materials and methods section. The experiments were performed in triplicate (one representative experiment; $n = 5$ experiments). Statistical significance (p -values) compare normal glucose untreated vs. CRT at peak activity of 1.0 ng/mL ($**p \leq 0.0001$); high glucose untreated vs. CRT at peak activity (50 ng/mL) ($***p \leq 0.0004$). (C) Concentration-dependent directed migration of human fibroblasts. CRT induces concentration-dependent migration of human fibroblasts grown in normal or high glucose in a chamber assay. Increasing doses of CRT (1.0–100 ng/mL) were added to the lower chambers, the cells applied to the membranes, and after 4 hours, the number of cells that migrated through the membrane counted as described in the materials and methods section. Experiments were performed in triplicate ($n = 5$ experiments). Statistical significance (p -values) compare normal glucose with high glucose at peak activity of CRT for normal (10 ng/mL) ($*p \leq 0.030$); normal untreated vs. CRT (10 ng/mL) ($**p \leq 0.033$); high glucose untreated vs. CRT at peak activity (10 ng/mL) ($***p \leq 0.007$). FGF positive control is at 5 ng/mL.

fibroblasts isolated from db/db and wt mice were remarkably morphologically different. In contrast to the poor proliferative response of the db/db fibroblasts to CRT in vitro, these cells showed similar sensitivity as the wt fibroblasts in the migratory response to CRT. However, the db/db fibroblasts did not fill in the wound defect in the scratch plate assay to the same extent as the wt fibroblasts (57.6% vs. 87.4%), and they

required twice as much CRT for this peak response. Similarly, the magnitude of the chemotactic response was decreased in the db/db compared with the wt cells (2.8-fold vs. 4.2-fold over untreated control) in the chamber assay.

Similar to the db/db mouse fibroblasts, human fibroblasts in high glucose (i.e., naturally or experimentally impaired) responded less well to CRT stimulation of proliferation than

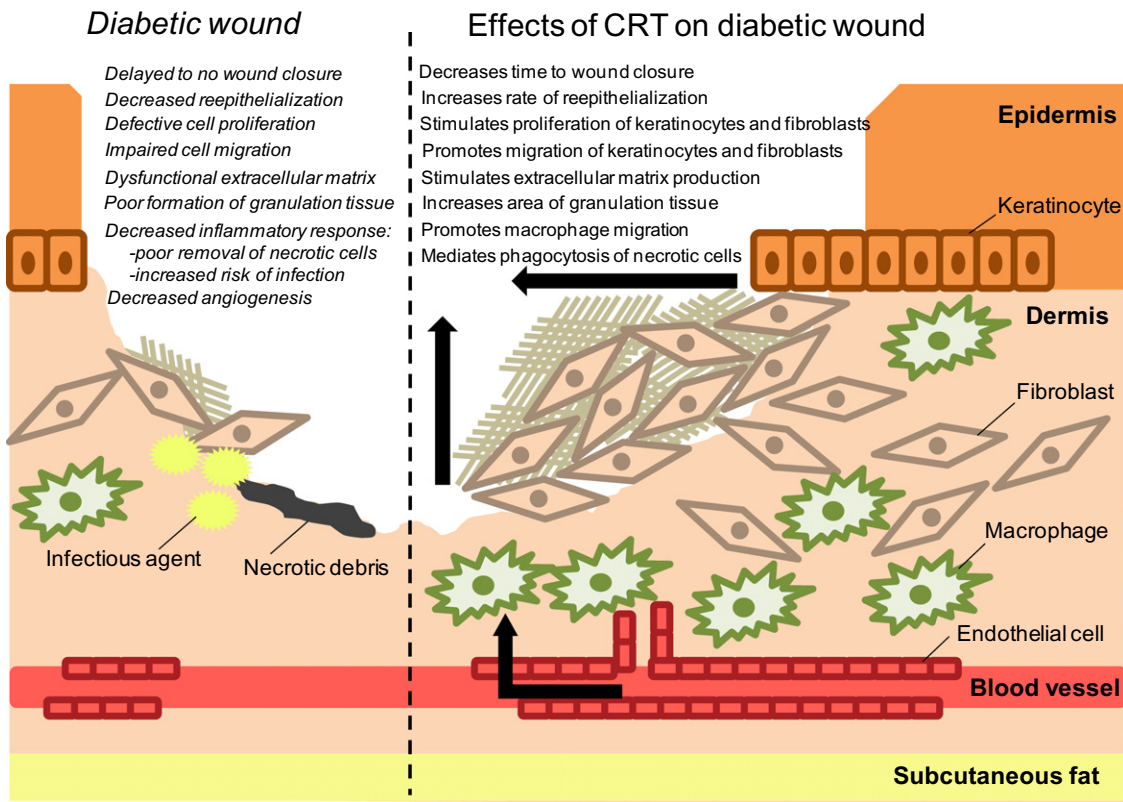


Figure 6. Diagram depicting the effects of calreticulin on specific defects of healing diabetic wounds.

their wt/normal counterparts. This might be related to high lactate in these cells as it has been shown that fibroblasts directly isolated from diabetic wounds produce higher levels of lactate compared with nondiabetic fibroblasts, and treatment of the latter with high glucose similarly induced high lactate in association with decreased proliferation.^{23,38} In contrast, human fibroblasts grown in high compared with normal glucose levels were only moderately affected in their migratory response in the in vitro wound healing scratch plate assay (88% vs. 92% wound closure), but the cells were less sensitive to CRT, requiring 50 times more CRT for this peak response; the chamber assay showed a similar decreased response as the fibroblasts in high glucose gave 54% less cells migrating through the membranes with 15 times more CRT. It has been shown that fibroblasts isolated from the nonhealing edge of a chronic wound migrate more poorly than those derived from the healing edge.^{21,39} This suggests that the molecular changes in the cells associated with the systemic effects of diabetes might be reversible. Conversely, the fact that db/db fibroblasts grown in media with normal plasma levels of glucose are less responsive to CRT than wt, particularly in their ability to proliferate, implicates the metabolic and molecular defects associated with diabetes are an inherent reflection of systemic disease and not readily reversible. Taken together, our in vitro results suggest that CRT might rescue the functional defects of fibroblasts in a chronic diabetic wound particularly with respect to their migration into

and throughout the wound bed to facilitate production of a more normal GT to enable improved healing of diabetic wounds.

Notably, the responses to topical CRT in vivo were more robust than in vitro (mouse db/db cells and human in high glucose). The blunted proliferative response in vitro is not consistent with the in vivo studies in which CRT clearly induced proliferation of fibroblasts in both the diabetic (db/db) mouse wound healing model herein and the cortisone-treated porcine model of impaired repair¹⁰ as shown by the cellularity of the neodermis and staining for proliferation markers in both studies. This suggests that other factors present in vivo can act synergistically with CRT or affect other dermal cells to produce growth stimulatory cytokines and growth factors to stimulate proliferation of fibroblasts, thereby contributing to the marked cellular GT and enhanced wound healing observed and/or CRT functionally improves other biological activities defective in diabetic wound repair not tested in our in vitro assays. Interestingly, the migratory response to CRT was similar to FGF suggesting that CRT might be as potent a chemoattractant for fibroblasts as this specific factor.

The mechanisms involved in partitioning CRT into various cellular compartments to perform its diverse intracellular and extracellular functions that span from the ER to the cytoplasm, cell surface, and extracellular space have been elusive. CRT is a nonglycosylated protein and is therefore not

secreted from the cell by conventional routes. Despite much investigation, the exit route from cells is still unknown.⁹ Recently, one report suggested an aminophospholipid translocase, a calcium, and a PS-dependent flip-out mechanism from the inner plasma membrane to the cell surface.⁴⁰ With respect to wound healing, the mechanical release of CRT upon cell death in the injured hypoxic wound microenvironment contributes to the extracellular presence and physiological action of CRT in wound healing. Interestingly, other intracellular ER and cytosolic chaperone proteins such as heat shock protein (Hsp)-90 α , which exits cells by an exosomal route, and Hsp-60, Hsp-47, Hsp-70, and Gp96, can induce cellular functions that regulate wound healing.^{9,41} The intracellular chaperone high-mobility group box (HMGB) 1 has been shown to be deficient in human and mouse models of diabetic wound healing and topical application of this protein rescued specific defects related to diabetic wound healing with no effect on normal cutaneous healing.⁴² Notably, HMGB1 is released during necrotic and apoptotic cell death as a pro-inflammatory factor,^{43,44} and CRT translocates to the cell surface from the ER prior to Hsp-70, Hsp-90, and HMGB1 release during immunogenic cancer cell death.⁴⁵ Thus, a cascade of release of intracellular chaperones appears to play a greater role than previously known in biological activities and cellular processes including phagocytosis, cell migration and proliferation, the immune response, cancer, and tissue repair.^{9,10,19,20,46}

Cell surface CRT lacks a transmembrane domain and therefore does not itself engage in signal transduction. To date, only one receptor, the low-density LRP1 has been identified as a signaling moiety for CRT-mediated extracellular functions.⁹ Both focal adhesion disassembly and resistance to anoikis are dependent on LRP1 and the matrix protein TSP-1 in a coreceptor complex with CRT.^{18,47,48} CRT likely regulates wound healing through both its ER chaperone activity and extracellular induction of functions through LRP1 and likely unidentified receptor signaling via classic intracellular signaling intermediates for target gene activation. Indeed, CRT is a requisite ER chaperone for integrins involved in cell migration, as well as collagen transcription and processing, and fibronectin synthesis, and release.^{12,49,50} We showed in vitro that exogenous CRT dose-dependently induces these proteins in fibroblasts (unpublished data). Therefore, our data underscore a dual role (i.e., intracellular and extracellular) for CRT and other chaperone proteins in a variety of cellular functions. Translating our data using the db/db mouse model of impaired wound healing and fibroblasts derived from these animals, exogenous CRT ameliorates dysfunction characteristic of poor healing wounds of patients with diabetes mellitus, particularly DFUs (Figure 6). Therefore, our studies support a novel therapeutic application of CRT to compensate for impaired healing of diabetic wounds.

ACKNOWLEDGMENTS

These studies were supported in part by Calretex LLC of Cahn Medical Technologies, Tenafly, NJ, and Calregen, Inc, Mamaroneck, NY. We are grateful to Emily Savoca for her expert help with editing this manuscript.

Conflict of Interest: No conflicts of interest exist among the authors and these entities.

REFERENCES

- Clark RA, Ghosh K, Tonnesen MG. Tissue engineering for cutaneous wounds. *J Invest Dermatol* 2007; 127: 1018–29.
- Brem H, Sheehan P, Boulton AJ. Protocol for treatment of diabetic foot ulcers. *Am J Surg* 2004; 187: 1S–10S.
- Sweitzer SM, Fann SA, Borg TK, Baynes JW, Yost MJ. What is the future of diabetic wound care? *Diabetes Educ* 2006; 32: 197–210.
- Liu ZJ, Velazquez OC. Hyperoxia, endothelial progenitor cell mobilization, and diabetic wound healing. *Antioxid Redox Signal* 2008; 10: 1869–82.
- Singer AJ, Clark RA. Cutaneous wound healing. *N Engl J Med* 1999; 341: 738–46.
- Bjarnsholt T, Kirketerp-Moller K, Jensen PO, Madsen KG, Phipps R, Krogfelt K, Hoiby N, Givskov M. Why chronic wounds will not heal: a novel hypothesis. *Wound Rep Reg* 2008; 16: 2–10.
- Ochoa O, Torres FM, Shireman PK. Chemokines and diabetic wound healing. *Vascular* 2007; 15: 350–5.
- Michalak M, Groenendyk J, Szabo E, Gold LI, Opas M. Calreticulin, a multi-process calcium-buffering chaperone of the endoplasmic reticulum. *Biochem J* 2009; 417: 651–66.
- Gold LI, Eggleton P, Sweetwyne MT, Van Duyn LB, Greives MR, Naylor SM, Michalak M, Murphy-Ullrich JE. Calreticulin: non-endoplasmic reticulum functions in physiology and disease. *FASEB J* 2010; 24: 665–83.
- Nanney LB, Woodrell CD, Greives MR, Cardwell NL, Pollins AC, Bancroft TA, Chesser A, Michalak M, Rahman M, Siebert JW, Gold LI. Calreticulin enhances porcine wound repair by diverse biological effects. *Am J Pathol* 2008; 173: 610–30.
- Sweetwyne MT, Paller MA, Lu A, Van Duyn Graham L, Murphy-Ullrich JE. The calreticulin-binding sequence of thrombospondin 1 regulates collagen expression and organization during tissue remodeling. *Am J Pathol* 2010; 177: 1710–24.
- Van Duyn Graham L, Sweetwyne MT, Paller MA, Murphy-Ullrich JE. Intracellular calreticulin regulates multiple steps in fibrillar collagen expression, trafficking, and processing into the extracellular matrix. *J Biol Chem* 2010; 285: 7067–78.
- Bedard K, Szabo E, Michalak M, Opas M. Cellular functions of endoplasmic reticulum chaperones calreticulin, calnexin, and ERp57. *Int Rev Cytol* 2005; 245: 91–121.
- Szewczenko-Pawlikowski M, Dziak E, McLaren MJ, Michalak M, Opas M. Heat shock-regulated expression of calreticulin in retinal pigment epithelium. *Mol Cell Biochem* 1997; 177: 145–52.
- Waser M, Mesaeli N, Spencer C, Michalak M. Regulation of calreticulin gene expression by calcium. *J Cell Biol* 1997; 138: 547–57.
- Elton CM, Smethurst PA, Eggleton P, Farndale RW. Physical and functional interaction between cell-surface calreticulin and the collagen receptors integrin $\alpha 2\beta 1$ and glycoprotein VI in human platelets. *Thromb Haemost* 2002; 88: 648–54.
- McDonnell JM, Jones GE, White TK, Tanzer ML. Calreticulin binding affinity for glycosylated laminin. *J Biol Chem* 1996; 271: 7891–4.
- Goicoechea S, Orr AW, Paller MA, Eggleton P, Murphy-Ullrich JE. Thrombospondin mediates focal adhesion disassembly through interactions with cell surface calreticulin. *J Biol Chem* 2000; 275: 36358–68.

19. Gardai SJ, McPhillips KA, Frasca SC, Janssen WJ, Starefeldt A, Murphy-Ullrich JE, Bratton DL, Michalak M, Henson PM. Cell-surface calreticulin initiates clearance of viable or apoptotic cells through trans-activation of LRP on the phagocyte. *Cell* 2005; 123: 321–34.
20. Chao MP, Jaiswal S, Weissman-Tsukamoto R, Alizadeh AA, Gentles AJ, Volkmer J, Weiskopf K, Willingham SB, Raveh T, Park CY, Majeti R, Weissman IL. Calreticulin is the dominant pro-phagocytic signal on multiple human cancers and is counterbalanced by CD47. *Sci Transl Med* 2010; 2: 63ra94.
21. Brem H, Tomic-Canic M. Cellular and molecular basis of wound healing in diabetes. *J Clin Invest* 2007; 117: 1219–22.
22. Lerman OZ, Galiano RD, Armour M, Levine JP, Gurtner GC. Cellular dysfunction in the diabetic fibroblast: impairment in migration, vascular endothelial growth factor production, and response to hypoxia. *Am J Pathol* 2003; 162: 303–12.
23. Hehenberger K, Heilborn JD, Brismar K, Hansson A. Inhibited proliferation of fibroblasts derived from chronic diabetic wounds and normal dermal fibroblasts treated with high glucose is associated with increased formation of l-lactate. *Wound Rep Reg* 1998; 6: 135–41.
24. Conway EM, Liu L, Nowakowski B, Steiner-Mosonyi M, Ribeiro SP, Michalak M. Heat shock-sensitive expression of calreticulin. In vitro and in vivo up-regulation. *J Biol Chem* 1995; 270: 17011–16.
25. Michaels JT, Dobryansky M, Galiano RD, Bhatt KA, Ashinoff R, Ceradini DJ, Gurtner GC. Topical vascular endothelial growth factor reverses delayed wound healing secondary to angiogenesis inhibitor administration. *Wound Rep Reg* 2005; 13: 506–12.
26. Galiano RD, Michaels J, Dobryansky M, Levine JP, Gurtner GC. Quantitative and reproducible murine model of excisional wound healing. *Wound Rep Reg* 2004; 12: 485–92.
27. Qi W, Poronnik P, Young B, Jackson CJ, Field MJ, Pollock CA. Human cortical fibroblast responses to high glucose and hypoxia. *Nephron Physiol* 2004; 96: 121–9.
28. Deveci M, Gilmont RR, Dunham WR, Mudge BP, Smith DJ, Marcelo CL. Glutathione enhances fibroblast collagen contraction and protects keratinocytes from apoptosis in hyperglycaemic culture. *Br J Dermatol* 2005; 152: 217–24.
29. Maruyama K, Asai J, Ii M, Thorne T, Losordo DW, D'Amore PA. Decreased macrophage number and activation lead to reduced lymphatic vessel formation and contribute to impaired diabetic wound healing. *Am J Pathol* 2007; 170: 1178–91.
30. Boulton AJ, Meneses P, Ennis WJ. Diabetic foot ulcers: a framework for prevention and care. *Wound Rep Reg* 1999; 7: 7–16.
31. Younes NA, Albsoul AM, Awad H. Diabetic heel ulcers: a major risk factor for lower extremity amputation. *Ostomy Wound Manage* 2004; 50: 50–60.
32. Falanga V. Wound healing and its impairment in the diabetic foot. *Lancet* 2005; 366: 1736–43.
33. Michaels J, Churgin SS, Blechman KM, Greives MR, Aarabi S, Galiano RD, Gurtner GC. db/db Mice exhibit severe wound-healing impairments compared with other murine diabetic strains in a silicone-splinted excisional wound model. *Wound Rep Reg* 2007; 15: 665–70.
34. Schmidt-Ullrich R, Paus R. Molecular principles of hair follicle induction and morphogenesis. *Bioessays* 2005; 27: 247–61.
35. Ito M, Yang Z, Andl T, Cui C, Kim N, Millar SE, Cotsarelis G. Wnt-dependent de novo hair follicle regeneration in adult mouse skin after wounding. *Nature* 2007; 447: 316–20.
36. Fathke C, Wilson L, Shah K, Kim B, Hocking A, Moon R, Isik F. Wnt signaling induces epithelial differentiation during cutaneous wound healing. *BMC Cell Biol* 2006; 7: 4.
37. Loot MA, Kenter SB, Au FL, van Galen WJ, Middelkoop E, Bos JD, Mekkes JR. Fibroblasts derived from chronic diabetic ulcers differ in their response to stimulation with EGF, IGF-I, bFGF and PDGF-AB compared to controls. *Eur J Cell Biol* 2002; 81: 153–60.
38. Hehenberger K, Kratz G, Hansson A, Brismar K. Fibroblasts derived from human chronic diabetic wounds have a decreased proliferation rate, which is recovered by the addition of heparin. *J Dermatol Sci* 1998; 16: 144–51.
39. Brem H, Golinko MS, Stojadinovic O, Kodra A, Diegelmann RF, Vukelic S, Entero H, Coppock DL, Tomic-Canic M. Primary cultured fibroblasts derived from patients with chronic wounds: a methodology to produce human cell lines and test putative growth factor therapy such as GMCSF. *J Transl Med* 2008; 6: 75.
40. Tarr JM, Young PJ, Morse R, Shaw DJ, Haigh R, Petrov PG, Johnson SJ, Winyard PG, Eggleton P. A mechanism of release of calreticulin from cells during apoptosis. *J Mol Biol* 2012; 401: 799–812.
41. Cheng CF, Fan J, Fedesco M, Guan S, Li Y, Bandyopadhyay B, Li Y, Bright AM, Yerushalmi D, Liang M, Chen M, Han YP, Woodley DT, Li W. Transforming growth factor alpha (TGFalpha)-stimulated secretion of HSP90alpha: using the receptor LRP-1/CD91 to promote human skin cell migration against a TGFbeta-rich environment during wound healing. *Mol Cell Biol* 2008; 28: 3344–58.
42. Straino S, Di Carlo A, Mangoni A, De Mori R, Guerra L, Maurelli R, Panacchia L, Di Campli C, Uccioli L, Biglioli P, Bianchi ME, Capogrossi MC, Germani A. High-mobility group box 1 protein in human and murine skin: involvement in wound healing. *J Invest Dermatol* 2008; 128: 1545–53.
43. Scaffidi P, Misteli T, Bianchi ME. Release of chromatin protein HMGB1 by necrotic cells triggers inflammation. *Nature* 2002; 418: 191–5.
44. Bell CW, Jiang W, Reich CF 3rd, Pisetsky DS. The extracellular release of HMGB1 during apoptotic cell death. *Am J Physiol Cell Physiol* 2006; 291: C1318–25.
45. Tesniere A, Apetoh L, Ghiringhelli F, Joza N, Panaretakis T, Kepp O, Schlemmer F, Zitvogel L, Kroemer G. Immunogenic cancer cell death: a key-lock paradigm. *Curr Opin Immunol* 2008; 20: 504–11.
46. Obeid M. Anticancer activity of targeted proapoptotic peptides and chemotherapy is highly improved by targeted cell surface calreticulin-inducer peptides. *Mol Cancer Ther* 2009; 8: 2693–707.
47. Orr AW, Elzie CA, Kucik DF, Murphy-Ullrich JE. Thrombospondin signaling through the calreticulin/LDL receptor-related protein co-complex stimulates random and directed cell migration. *J Cell Sci* 2003; 116 (Pt 14): 2917–27.
48. Pallero MA, Elzie CA, Chen J, Mosher DF, Murphy-Ullrich JE. Thrombospondin 1 binding to calreticulin-LRP1 signals resistance to anoikis. *FASEB J* 2008; 22: 3968–79.
49. Coppolino MG, Dedhar S. Ligand-specific, transient interaction between integrins and calreticulin during cell adhesion to extracellular matrix proteins is dependent upon phosphorylation/dephosphorylation events. *Biochem J* 1999; 340 (Pt 1): 41–50.
50. Papp S, Szabo E, Kim H, McCulloch CA, Opas M. Kinase-dependent adhesion to fibronectin: regulation by calreticulin. *Exp Cell Res* 2008; 314: 1313–26.

Supporting Information

Additional Supporting Information may be found in the online version of this article:

Figure S1. Topical application of calreticulin (CRT) accelerates wound healing in diabetic (db/db) mice histology of wounds shown at 28 days postwounding. Wounds were prepared as described in materials and methods section and stained with hematoxylin/eosin (H&E). CRT-treated wounds contained hair follicles in the original wound bed, which is marked by upward facing green arrows denoting the original cut into the *panniculus carnosus*. Magnification = 40× (scale bar = 396 μM) ($n = 6$ mice/twowounds/mouse).

Figure S2. Spatial and temporal dynamic expression of calreticulin is during diabetic murine wound healing. As an ER chaperone protein that is up-regulated under stress conditions,¹³ we proposed that CRT should play an important physiological role in the wound repair process. Experimental wounds were created, treated, and excised, as described in the materials and methods section. The tissue was fixed in 10% buffered formalin and slides prepared. Immunostaining for endogenous CRT in buffer-treated wounds was determined at 4 and 10 days after wounding by immunohistochemical analysis (IHC) using a polyclonal goat anti-rabbit CRT, as described.¹⁰ The tissues were blocked with normal rabbit serum (S5000; Vector Laboratories, Burlingame, CA) in Tris-buffered Saline (TBS) for 20 minutes. CRT antibody (1 : 1000; pantropic goat anticalreticulin; from M. Michalak, University of Alberta, Edmonton, Canada) in Tris-buffered saline (TBS) containing 0.5% bovine serum albumin (blocking buffer), was incubated with the slides over night at 4 °C. The secondary antibody was biotinylated rabbit anti-goat IgG (Vector, BA5000). The Vector kit PK6200 and the substrate,

0.05% 3,3-diaminobenzidine HCl (DAB, Sigma, D5637) was used for detection (brown stain) and the slides were counterstained with hematoxylin (Fisher CS401-1D). CRT is spatially and temporally expressed throughout the wound healing process in the diabetic mice. In addition, compared with the untreated control (panel A), the positive control, VEGF, appears to increase CRT immunostaining in the granulation tissue (GT) and epithelium (EP) shown at day 4 postwounding (panel B). CRT continues to be up-regulated in the granulation tissue and all layers of the epidermis at 10 days postwounding (compare panel C with D). The insert in panel C shows no immunostaining of the normal rabbit serum (NRS) control. CRT is not present in the migrating epithelium (black arrows; ME) in nontreated (panel G) or VEGF-treated animals (panels B,D). CRT is highly expressed in the epidermis of unwounded skin (panel E), shows less expression at day 4 postwounding (panel A) and is weakly expressed in the hypertrophic epidermis (blue arrow) of the wound by day 10 postinjury (panel C). As shown in panels C and D, CRT is not expressed in the proliferating basal and suprabasal layers of the epidermis (green arrows) whereas interestingly, these basal keratinocytes proliferate in response to topical CRT (Figure 2B). Red arrow = putative macrophages in panels A and F; blue arrow = hypertrophic epidermis (EP) in panel C; black arrow = migrating epithelium (ME) in panels D and G; Green arrow shows lack of immunostaining in basal epithelium in panels C and D. Granulation tissue (GT). Magnification: panels A–E: 160× (scale bar = 96 μM; panels F, G: 320× (scale bar = 48 μM; NRS control, panel C: magnification = 110× (scale bar = 144 μM).

Please note: Wiley-Blackwell is not responsible for the content or functionality of any supporting materials supplied by the authors. Any queries (other than missing material) should be directed to the corresponding author for the article.